Plasma characterization at comet 67P between 2 and 4 AU from the Sun with the RPC-MIP instrument

Gaëtan Wattieaux, Pierre Henri, Nicolat Gilet, Xavier Vallières, Jan Deca

HAL Id: insu-02610363
https://insu.hal.science/insu-02610363

Submitted on 2 Jun 2020

Plasma characterization at comet 67P between 2 and 4 AU from the Sun with the RPC-MIP instrument

Gaëtan Wattieaux[1], Pierre Henri[2,3], Nicolas Gilet[2], Xavier Vallières[2], and Jan Deca[4,5,6]

[1] Laboratoire Plasma et Conversion d'Energie (LAPLACE), Université de Toulouse, CNRS, 31062 Toulouse, France
e-mail: gaetan.wattieaux@laplace.univ-tlse.fr
[2] Laboratoire de Physique et Chimie de l'Environnement et de l'Espace (LPC2E), CNRS, 45071 Orléans, France
[3] Laboratoire Lagrange, OCA, CNRS, UCA, Nice, France
[4] Laboratory for Atmospheric and Space Physics (LASP), University of Colorado Boulder 3665 Discovery Drive, Boulder, CO 80303, USA
[5] Institute for Modeling Plasma, Atmospheres and Cosmic Dust, NASA/SSERVI, California 94035, USA
[6] Laboratoire Atmosphères, Milieux, Observations Spatiales (LATMOS), Université de Versailles à Saint Quentin, 78280 Guyancourt, France

May 12, 2020

ABSTRACT

The plasma of comet 67P/Churyumov–Gerasimenko is analyzed based on the RPC-MIP mutual impedance probe data of the Rosetta mission. Numerical simulations of the RPC-MIP instrumental response considering two populations of electrons were fit on experimental responses acquired from January to September 2016 to extract the electron densities and temperatures. A time-tracking of the plasma parameters was performed, leading to the identification of a cold and a warm population of electrons during the period of interest. The respective densities and temperatures lie in the ranges $[100\,;\,1000]\,\mathrm{cm}^{-3}$ and $[0.05\,;\,0.3]$ eV for the cold electrons and in the ranges $[50\,;\,500]\,\mathrm{cm}^{-3}$ and $[2\,;\,10]$ eV for the warm electrons. Warm electrons most of the time made up between 10% and 30% of the whole population, while the temperature ratio between warm and cold electrons lay mostly between 30 and 70 during the period we studied. The fluctuation range of the plasma parameters, that is, the electron densities and temperatures, appears to have remained rather constant during the last nine months of the mission. We take the limitations of the instrument that are due to the experimental noise into account in our discussion of the results.

1. Introduction

The Rosetta Plasma Consortium Mutual Impedance Probe (RPC-MIP) instrument (Trotignon et al. (2007)) on board the Rosetta orbiter spacecraft consisted of a mutual impedance probe and was used to characterized the cometary plasma of comet 67P/Churyumov–Gerasimenko (67P). Electrostatic active probes like this have been successfully involved in terrestrial ionospheric and space plasma analysis (Grard 1969; Storey et al. 1969; Beghin & Debrie 1972; Chasseriaux et al. 1972; Rooy et al. 1972; Pottelette et al. 1975; Décréau et al. 1978; Pottelette & Storey 1981; Beghin et al. 1982; Beghin 1995; Grard 1997; Storey 1998; Geiswiller et al. 2001; Béghin et al. 2005). RPC-MIP was made of four electric antennas, two of which were used as transmitters, and the other two were used as receivers (Trotignon et al. 2007). A sine electric potential was applied on the transmitters, which induced a potential difference between the receivers, and a frequency sweep enabled studying the dielectric medium that surrounded the probe (the plasma and the positive ion sheath). The spectral power of the potential difference between the receivers is referred to as the response of the probe. It is expected that the electron energy distribution function (eedf) can be characterized based on the response of the probe, but this inverse problem may have multiple solutions. In order to constrain the solutions, a double Maxwellian eedf involving a cold and a warm electron population is assumed at 67P. A recent electrostatic simulation of the probe op-

erated in such a plasma (Wattieaux, G. et al. 2019) has shown that the instrumental response of the RPC-MIP experiment is not compatible with a single Maxwellian electron population, and it has provided simulated responses in accordance with experimental responses when two electron populations with different temperatures are considered. The existence of two different electron populations in the cometary plasma agrees with observations from the RPC-LAP dual Langmuir probe of Rosetta (Eriksson et al. 2017) and with previous cometary measurements made during the flyby at comet 21P/Giacobini-Zinner of the International Cometary Explorer (ICE) (Meyer-Vernet et al. 1986). Wattieaux, G. et al. (2019) also underlined the influence of the positive ion sheath that surrounded the probe and the Rosetta spacecraft when they were exposed to the cometary plasma and were consequently negatively charged (Odelstad et al. 2015).

We here focus on the last nine months of the Rosetta cometary operations (January to September 2016) because the response of the RPC-MIP probe exhibited a clear plasma signature that emerged from the noise more often than during the first half of Rosetta cometary operations. This is particularly noticeable during the last two months of operations when the spacecraft approached the comet nucleus. The response of the probe in the different operating modes was studied in Gilet et al. (2019b).

2. Model, fitting process, and limits of the diagnostic

We here use the mutual impedance experiment model developed and validated on RPC-MIP data in Wattieaux, G. et al. (2019), which takes into account (i) the geometry of the Rosetta spacecraft as well as the RPC-MIP quadrupolar antenna, (ii) the ion sheath surrounding the spacecraft and the experiment because of the negative spacecraft-charging reported at Rosetta (Odelstad et al. 2015), and (iii) two different electron populations modeled by two Maxwellian distribution functions in the plasma dielectric function (Gilet et al. 2017). The spectral power of the RPC-MIP experiment is referred to as the response of the probe (in dB units) $P_{dB} = 10 \log_{10} \left(20 \, |\Delta V_R|^2 \right)$, where ΔV_R is the voltage drop between the receivers of the probe (in mV units) at a given frequency (Wattieaux, G. et al. (2019)).
The comparison of simulated with experimental responses provides four parameters that characterize the plasma eedf at comet 67P in terms of electron densities and temperatures. In the following, we assume n_c and n_h , which correspond to the density of cold and warm electron populations, respectively, while T_c and T_h correspond to the average temperatures of cold and warm electron populations, respectively. The overall electron density reads $n_{tot} = n_c + n_h$. The model is used in the so-called operational small Debye length (SDL) phase mode, that is, with both transmitters fed by oscillating currents in phase, and it requires five input parameters: the overall plasma frequency $f_{tot} = \sqrt{f_h^2 + f_c^2}$, where f_h and f_c are the plasma frequencies of the warm and cold electron populations, respectively; the thickness of the considered plasma sheath; the Debye length of the warm electron population (λ_{Dh}); the warm to overall electron density ratio ($\mu = n_h/n_{tot}$); and the warm to cold electron temperature ratio ($\tau = T_h/T_c$). The thickness of the considered plasma sheath has been shown to be no independent parameter because it scales as the warm population Debye length, which itself directly depends on the warm electron population density and temperature, so that the model is reduced to four degrees of freedom. The typical RPC-MIP experimental responses showing clear plasma signatures between January and September 2016 exhibit an antiresonance followed by a resonance at a higher frequency. Simulations have shown that the resonance occurs below the plasma frequency, while an antiresonance appears below the resonance frequency due to the occurrence of the sheath around the instrument (fig. 1 and more details in Wattieaux, G. et al. (2019)). The antiresonance and the resonance frequencies and amplitudes depend on all the input parameters. The experimental RPC-MIP responses also exhibited narrow peaks with smaller amplitude that are associated with interferences with the platform or other instruments. They were mostly present at 49 kHz harmonics, at 266 kHz, and 800 kHz. Such instrumental artifacts have been taken into account in this analysis by removing their signature as much as possible. Detailed information on these interferences and on the noise level of RPC-MIP mutual impedance responses is given in the RPC-MIP user guide (Henri et al. (2019)), which is available in the Planetary Science Archive RPC-MIP archive (Henri et al. (2018)).
A database of 1350 simulated RPC-MIP responses was generated with $\mu \in [0.1 \, ; 0.9]$ and $\tau \in [10 \, ; 100]$. We note that $\mu = 0$ or 1 corresponds to a single Maxwellian eedf that never provided simulation responses in accordance with experimental responses in which a clear plasma signature emerged from the noise. The sheath thickness $R \in [1 \, ; 1.7]$ m was set to the Debye length of the warm electron population λ_{Dh} , in agreement with the results from our previous study in Wattieaux, G. et al. (2019). The formulas used to derive the plasma parameters as well as the relative uncertainties associated with the discretization of the modeling input parameters (a step of 0.1 on μ, 10 on τ, and 5 cm on λ_{Dh} , and a resolution of 14 kHz on the experimental frequency) are displayed in Table 1.

Among the 2.4 millions experimental responses of the RPC-MIP instrument, which operated in the so-called SDL phase mode from January to September 2016, a selection algorithm identified about 875000 responses, at least 5% of whose points emerged from the experimental noise and were assumed to show a clear plasma signature. Nearly 65% of these selected responses have been found in accordance with one of the simulated responses taken from the database, with an average absolute difference below 1.5 dB (see fig. 1, which displays two experimental responses taken on 24 August 2016 that correspond to similar plasma parameters). The stacked bar charts in fig. 2 sort the daily responses into three categories. The first category contains responses in which no plasma signature emerged from the noise (1569509 responses from January to September 2016). The second category contains responses in which a clear plasma signature emerged from the noise, but that were not well fit by the simulations (305782 responses), and the last category gathers the responses in which a clear plasma signature emerged from the noise that were well fit by a simulated response in the database (569441 responses). A fit of the simulated response to the experimental data was considered good when the average absolute difference between them was lower than 1.5 dB. Above this value, the fitting was considered poor and was therefore discarded.
Previous simulations have found that the response of the probe is particularly sensitive to the electron temperature and density ratio in the vicinity of the plasma frequency, and to a lesser extent, to the sheath thickness, which is strongly related to the limit of the response level of the probe above the plasma frequency (Wattieaux, G. et al. 2019). It is therefore expected to observe experimental responses with a clear plasma signature that have not been computed during the build-up of the simulation database. Increasing the resolution on the temperature and density ratio in the simulations and computing the response of the probe for different sheath thickness appeared useless because the number of good fittings was high enough to follow the plasma evolution around 67P from January to September 2016. The heliocentric distance of the comet nucleus ranged between 2 and 4 AU during this time. However, the response amplitude of the probe decreases when λ_{Dh} and n_h/n_{tot} increase, which leads to experimental responses that can be hidden by the noise and thus reduces the available range of the plasma parameters that can be analyzed by the probe due to the noise. This is shown in fig. 3, where the available plasma parameter range corresponds to the white areas. Moreover, according to the simulations, a single Maxwellian eedf could have provided flat responses that could easily have been hidden by the experimental noise. Consequently, the

Parameter	Units	Formulas	Relative uncertainties
n_{tot}	cm^{-3}	$0.0124 \times (f_{tot}\,(\text{kHz}))^2$	$2\Delta f_{tot}/f_{tot} \approx \pm 1.56 \times (n_{tot})^{-1/2}$
n_h	cm^{-3}	$n_{tot} \times \mu$	$\Delta n_{tot}/n_{tot} + \Delta\mu/\mu$
n_c	cm^{-3}	$n_{tot} - n_h$	$\Delta n_{tot}/n_c + \Delta n_h/n_c$
T_h	eV	$0.018 \times (\lambda_{Dh}\,(\text{m}))^2 \times (n_h\,(\text{cm}^{-3}))$	$2 \times \Delta\lambda_{Dh}/\lambda_{Dh} + \Delta n_h/n_h$
T_c	eV	T_h/τ	$\Delta T_h/T_h + \Delta\tau/\tau^2 \approx \Delta T_h/T_h$

Table 1. Formulas used to derive the plasma parameters and their associated uncertainties. $\mu = n_h/n_{tot}$. $\tau = T_h/T_c$. The uncertainties due to the discretization of the parameters are $\Delta f_{tot} = \pm 7\text{kHz}$, $\Delta\mu = \pm 0.05$, $\Delta\tau = \pm 5$, and $\Delta\lambda_{Dh} = \pm 2.5\text{cm}$.

1.5 million experimental responses in which no plasma signature emerged from the noise were acquired in a plasma environment that was beyond the range of the RPC-MIP instrument, very likely because the plasma density was too low and/or the electron temperature associated with a too large sheath thickness around the probe was too high (e.g., $\lambda_{Dh} > 2\,\text{m}$), and also perhaps because of the occurrence of a single Maxwellian eedf. We also note that in some operational modes, the spectra telemetered from RPC-MIP corresponds to the average of different individual spectra acquired successively and averaged onboard. It is therefore also possible that the temporal or spatial dynamics of the cometary plasma between the different successive frequency sweeps, which were sometime separated by a few seconds and led to a single onboard-averaged telemetered spectrum, have evolved during the measurement so that the model, which was designed for a single and stable plasma configuration, cannot match the experimental averaged spectrum. It is also possible that the plasma might sometimes be characterized by a nontrivial eedf that would have been too different from a single or double Maxwellian and would also have led to experimental responses that were not expected after the simulation of the probe. We also note that simulations with a (single) Kappa eedf plasma (Gilet et al. 2019a) provided results that disagreed with the experimental responses acquired by the mutual impedance probe on board the Rosetta spacecraft during the period we considered here.

3. Locations of the Rosetta orbiter during the in situ measurements

The MIP instrument enabled us to access to the plasma properties in the close environment of the spacecraft: it provided in situ measurements of the plasma that surrounded both the spacecraft and its plasma sheath (i.e., a volume of several Debye lengths; typically, within a few meters to 10s of meters from the spacecraft). Figures 4 and 6 show the locations of the Rosetta orbiter from January to the end of September 2016 and on 21 and 24 August 2016 in the comet-centered solar equatorial-coordinate frame (CSEQ), which is defined as follows: the x-axis points from the comet to the Sun, the z-axis is the component of the solar north pole orthogonal to the x-axis, and the y-axis completes the right-handed reference frame, the origin of the coordinate system being the center of mass of the comet. Fig. 5 displays the spacecraft-comet distance and the Sun-spacecraft distance during the period we considered.
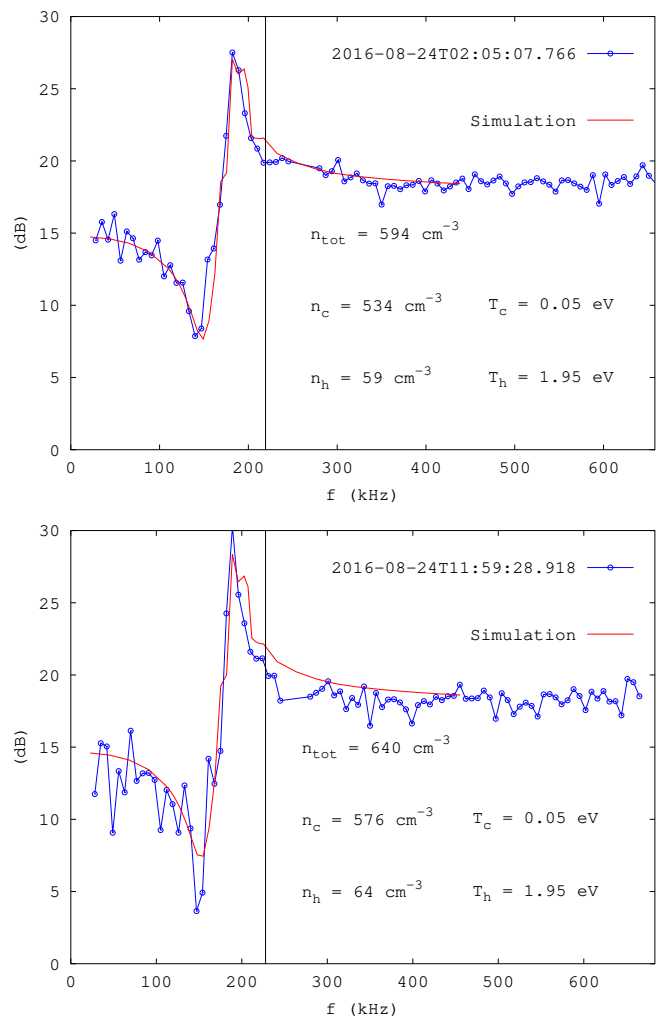

Fig. 1. Fitting our simulated responses on experimental responses taken on 24 August 2016. The average absolute difference between simulated and experimental responses is 0.6 dB (top panel) and 1.5 dB (bottom panel), respectively. The vertical line is located at the plasma frequency. The response maximum does not exactly correspond to the total plasma frequency because there are two electron populations. The experimental noise level estimate is 3 dB in the top panel and 4 dB in the bottom panel, according to the fluctuations of the responses above 300 kHz.

4. Reproducibility of the analysis

The trajectories of the spacecraft (fig. 6) as well as the values of the plasma parameters (fig. 7 and 8) were very similar on 21 August 2016 and on 24 August 2016. This provides a unique opportunity to verify both the stability of the cometary plasma and the reproducibility of the mutual
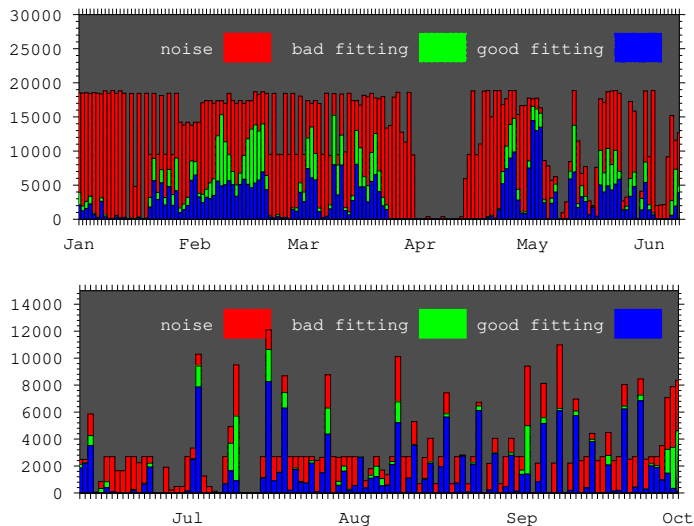
Fig. 2. Stacked bar charts representing the number of experimental responses in which no plasma signature emerged from the noise (red area, 1569509 responses), the number of experimental responses in which a plasma signature emerged from the noise but that were not well fit by the simulations (green area, 305782 responses), and the number of experimental responses in which a plasma signature emerged from the noise that were well fit by a simulation from the database (blue area, 569441 responses) between January and the end of September 2016.

impedance probe analysis in a very likely similar plasma environment.

5. Results

Under the model considered in this study (and even under simplified models), the instrumental responses of the RPC-MIP experiment that exhibited a clear plasma signature were never consistent with a single Maxwellian eedf. Fitting the simulated responses on the experimental responses led to the estimation of the electron densities n_{tot}, n_c, and n_h and of the electron temperatures T_c and T_h from January to the end of September 2016 with a time resolution that was occasionally as low as a few seconds. The evolution of these parameters is displayed in figs. 9 and 10, and their relative uncertainties are presented in fig. 11.

In the following, the cometary neutral density n_n measured by the Rosina/COPS experiment (Balsiger et al. 2007) is displayed together with the electron densities. It has been shown in previous studies that the plasma density around comet 67P is strongly correlated with the cometary neutral density as a result of the ionization of the latter by different processes, in particular, photoionization and electron-impact ionization (Vigren et al. 2016; Galand et al. 2016; Heritier, K. L. et al. 2018), with the latter dominating when the comet is typically above 3 A.U. from the Sun. This was
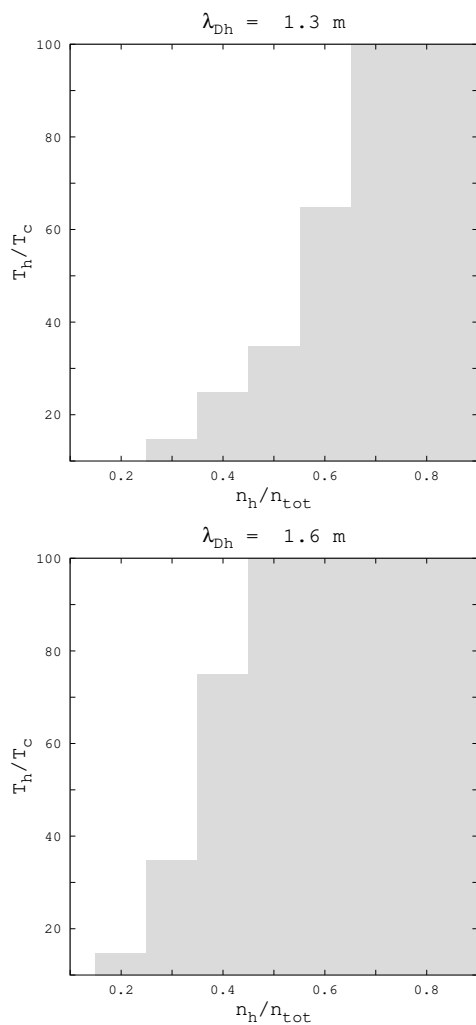

Fig. 3. Responses of the RPC-MIP instrument in which at least 5% of the points emerged from the noise (white area) and that did not reach 5% (gray area). The considered noise level is 4 dB. The instrument is simulated in full level emission SDL phase mode for two λ_{Dh} (Wattieaux, G. et al. (2019))

the case during the last months of cometary operations.

After the fitting process was carried out, the expected correlation between the plasma density and the cometary neutral density n_n was particularly visible for the cold electron density n_c and to a lesser extent for n_h, as shown in figs. 7 and 9. The overall electron density n_{tot} most of the time lay between 200 and 1000 cm^{-3} (fig. 9) at the spacecraft location when RPC-MIP was able to determine the cometary plasma density. This means that the plasma density might have reached values below 200 cm^{-3}, but it is very unlikely that it often exceeded 1000 cm^{-3}. Moreover, when measured, n_c and n_h mostly fluctuated in the respective ranges [100 ; 1000] cm^{-3} and [50 ; 500] cm^{-3} (figs. 9 and 13) with a high probability of finding the ratio n_h/n_{tot} in the range [0.1 ; 0.3] (figs. 12 and 13).

The electron temperature measurements from the MIP experiment in the ionized environment of comet 67P showed that the cold and warm electron temperatures were strongly correlated throughout the considered period (figs. 8 and 10). T_h most of the time lay in the range [2 ; 10] eV, while T_c fluctuated within [0.05 ; 0.3] eV (figs. 10 and 13), which is consistent with the RPC-LAP Langmuir probe measure-
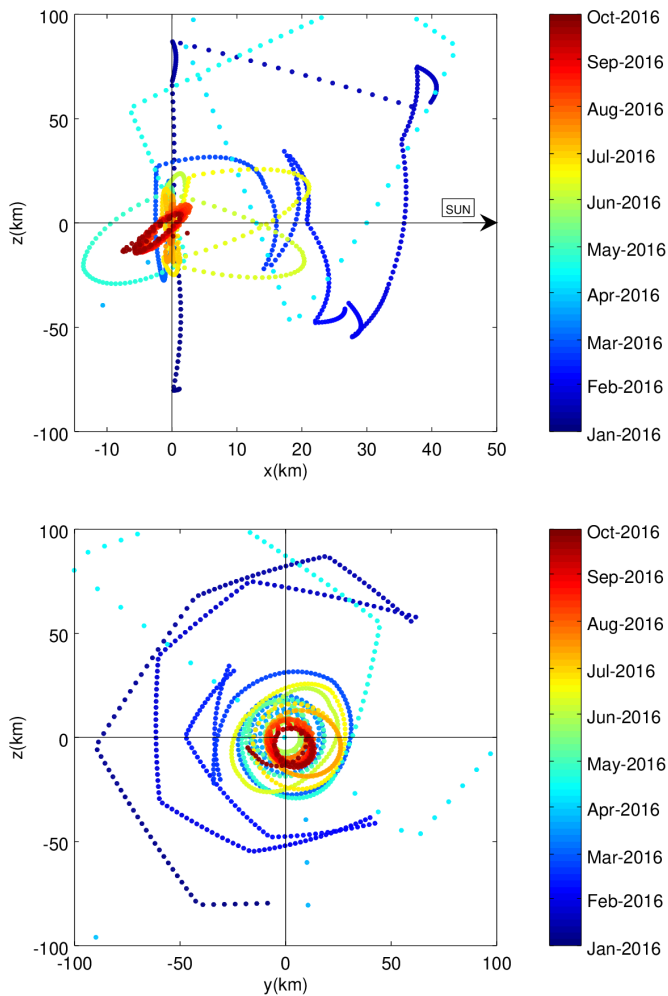
Fig. 4. Location of the Rosetta orbiter from January to September 2016 in the CSEQ coordinate frame showing the close-nucleus orbits during the last months of cometary operations. The center of mass of the cometary nucleus is located at the origin of the coordinate frame, and the x-axis points from the comet to the Sun. The time is color-coded. The time step is 4 hours. The spacecraft moved a few hundred kilometers away from the comet nucleus between 24 March and 17 April 2016, so that the corresponding locations are not displayed here.

ments at comet 67P (Eriksson et al. 2017). The ratio T_h/T_c is found to have fluctuated most of the time in the range $[30\,;\,60]$ (figs. 12 and 13).
Finally, the evolution of the cold and warm Debye length is displayed in fig. 14. The warm Debye length is found to have slowly increased from about 1.3 m to about 1.6 m as the comet moved away from the Sun. Figure 3 shows that due to the noise, the increase in warm Debye length significantly reduced the ability of the instrument to analyze plasma configurations with a high n_h/n_{tot} ratio. This might be the reason for the decrease in the ratio n_h/n_{tot} with time in fig. 12 because the evolution of this ratio appeared to be anticorrelated with the evolution of λ_{Dh}. In other words, plasmas with a higher proportion of warm electrons might have occurred without being detected by the instrument because of the noise, especially from July until the end of the cometary operations. The period between mid-March and mid-April 2016 corresponds to the so-called nightside excur-
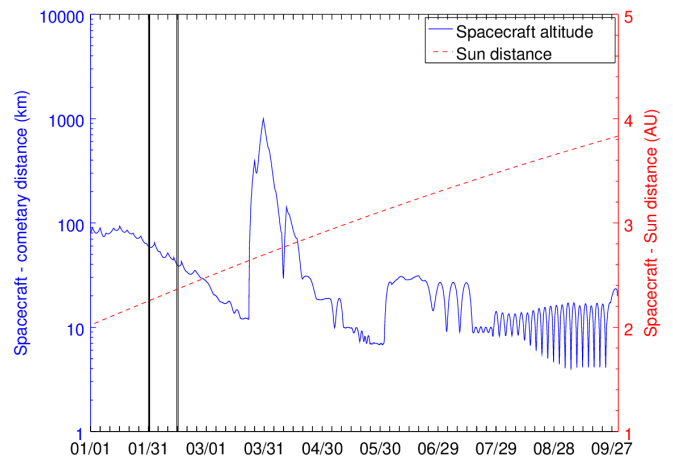

Fig. 5. Spacecraft-comet distance and Sun-spacecraft distance from January to September 2016. The vertical lines indicate when the spacecraft crossed the diamagnetic cavity (no magnetic field) that surrounded the comet nucleus (eight crossings on 31 January 2016, one crossing on 14 February 2016, and one crossing on 15 February 2016, each of them lasting less than 8 min).

sion of Rosetta: an operation of a few weeks during which the Rosetta orbiter moved away from the near-nucleus region to explore the first 1000 km of the nightside of the cometary coma (Behar, E. et al. (2018)), where the comet tail builds up (Volwerk, Martin et al. (2018)). This region is characterized by a plasma density much lower than that of the inner coma region. In plasmas with low densities (typically below $100\,\mathrm{cm}^{-3}$ in the SDL phased operation mode we used here), the RPC-MIP response flattened and the signal-to-noise ratio became too low to provide a reliable analysis of the cold and warm electron components in the plasma. This period of measurements was therefore discarded from our analysis.

6. Discussion

According to the assumptions considered in the modeling of the instrumental response of the mutual impedance probe MIP on board the Rosetta orbiter, two populations of electrons have been unambiguously identified and characterized in the cometary plasma of comet 67P. Their variations throughout the orbit of the Rosetta orbiter, both in terms of electron temperature and plasma density, on several-hour timescales were strongly associated with the inhomogeneously expanding cometary atmosphere, which itself is controlled by the illumination and composition of the irregular shape of the surface of the cometary nucleus. First, the approximately 12-hour-long rotation period of the cometary nucleus caused the spacecraft to travel through the cometary ionosphere, showing an associated 6-hour periodicity (fig 7), as reported in previous studies (Edberg et al. 2015). Second, larger temporal variations from a few days to weeks are associated with the variation in the location of the Rosetta orbiter in terms of latitude. It is noteworthy that the range of temperature fluctuations and of the densities remained stable throughout the nine months we analyzed (figs. 9, 10, and 13). The spacecraft locations in the close coma environment of comet 67P varied signif-
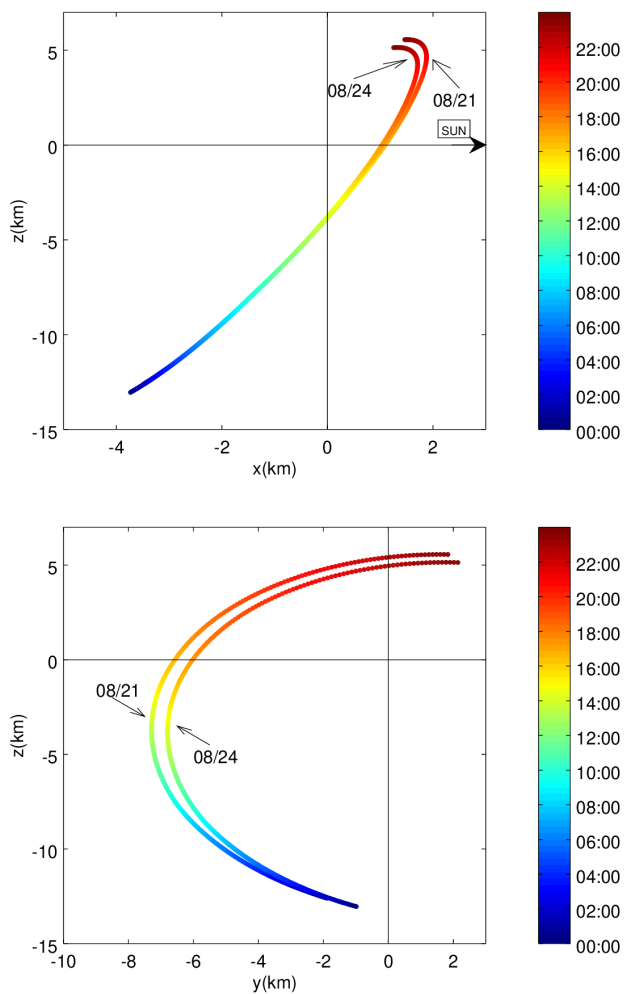
Fig. 6. Locations of the Rosetta orbiter in the CSEQ coordinate frame on 21 and 24 August 2016. The center of mass of the cometary nucleus is located at the origin of the coordinate frame, and the x-axis points from the comet to the Sun. The time is color-coded. The time step is 5 minutes.

Fig. 7. Evolution of the electron and neutral densities estimated on 21 August 2016 (top panel, 2732 samples) and on 24 August 2016 (bottom panel, 6130 samples). The gray curve is the neutral density measured by the Rosina experiment and normalized by $10^5 \, cm^{-3}$

icantly during the period of interest, as did the distance from the Sun (figs. 4 and 5).

Although collisions are not expected between the different electron populations because the electron-electron collision frequency is far too low to be significant in the cometary plasma, the correlation between the cold and warm electron populations (both in terms of density and temperature, fig. 9) nonetheless suggests a strong coupling of the two. This coupling might be indirect and mediated by the cometary neutral population, for example, through electron-neutral collisions.

It is important to recall that the results we presented here were determined in a plasma environment that sometimes was at the limit of the RPC-MIP instrument capabilities. Other plasma configurations may have occurred during the considered period that would have been hidden by the instrumental noise (see fig. 3). This corresponds to the red areas in fig. 2.

A particularly interesting result of this study is the well-defined regions of parameter space populated by the cold and warm electron populations reported in the right panel of Fig. 13. This shows no continuity between the two pop-
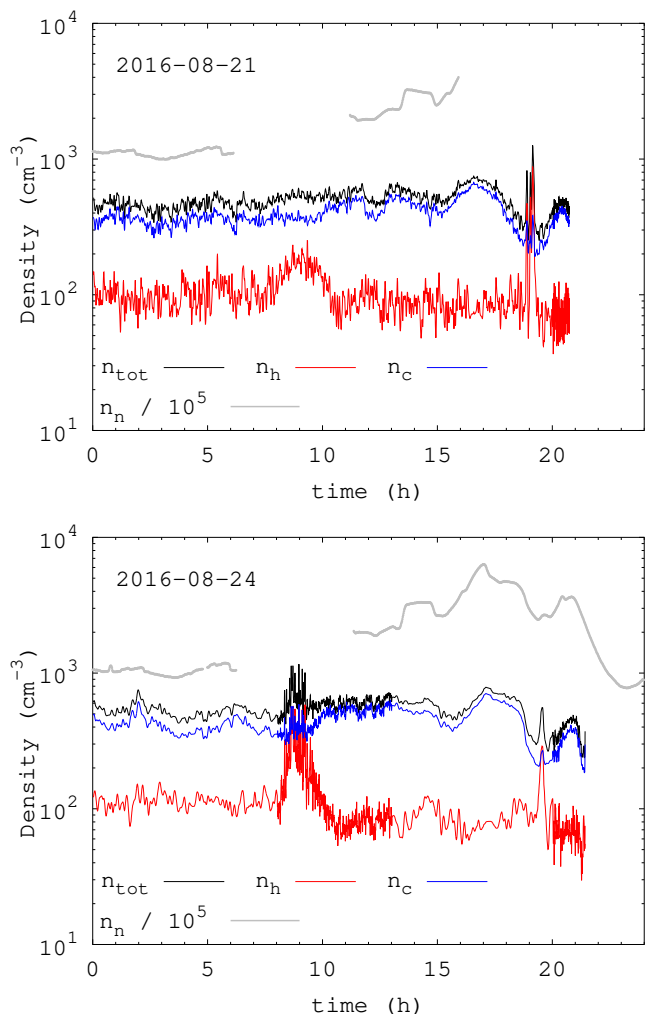
ulations. This suggests that when the electron cooling process occurs, it is particularly efficient and leads to two well-defined separated electron populations. The cold electron population is mostly observed for high enough densities, as might be expected if this population originated from electron-neutral collisions whose frequency increases with the neutral density of the comet, and therefore in dense (both neutral and plasma) regions.

The strong correlation we observed between the temperature and density of the warm electron population is of particular interest. It is unclear whether it reflects the result of (i) the collisionless expansion of the cometary plasma or (ii) the electron acceleration process in the corona, which is observed as heating.

First, the expansion of a plasma in vacuum has been extensively studied in the past, for instance, for laser-fusion plasmas (Murakami & Basko 2006; Beck & Pantellini 2008). Mass-loaded plasmas such as cometary plasma slightly differ from these plasmas because the ionization processes occur in the entire space around the comet. However, plasma expansion in vacuum might be a good first approximation of what might be expected at a comet, although cometary
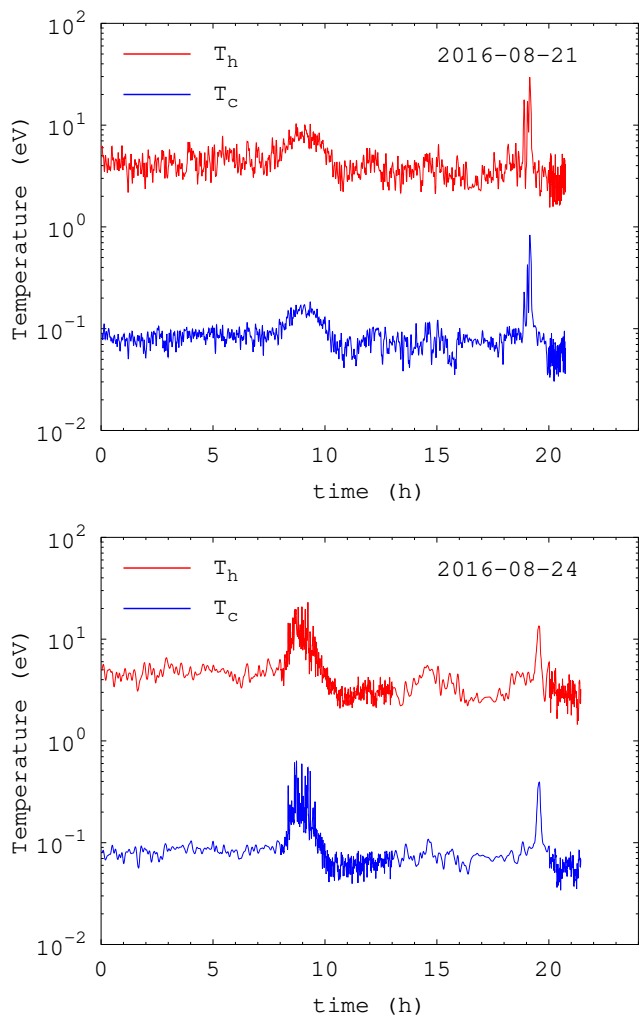
Fig. 8. Evolution of the electron temperatures on 21 August 2016 (top panel) and on 24 August 2016 (bottom panel).

electrons might be expected to behave more similarly to an isothermal plasma. This is not observed in the data.

Second, in order to assess the influence of the electron acceleration processes reported in previous studies that were shown to be associated with the action of the ambipolar electric field that in turn is associated with the large-scale electron pressure inhomogeneity in the cometary ionosphere (Madanian et al. 2016; Deca et al. 2017, 2019), we have used recent numerical simulations of the collisionless interaction of the solar wind with a comet to investigate the expected behavior of the electron temperature in the close cometary environment. The numerical simulation is described in Deca et al. (2019) and was performed using a full kinetic particle-in-cell simulator that enabled the authors to model the kinetic behavior of electrons. This model is collisionless, so that electron cooling is not included in the model. We computed the densities and temperatures directly from the electron distribution function (i.e., the macroparticles of the PIC simulation), considering the different electron populations present in our model, located close to the terminator plane where the Rosetta orbiter traveled. Figure 15 shows the expected behavior of electron temperature versus density according to the collisionless model for three different cases: first, by combining all electrons to a single popu-

lation to compute the total density and temperature (left panel); second, by considering only the electrons from the solar wind (middle panel); and third, by considering only electrons created close to the comet (right panel). Our PIC simulation shows that the behavior of the population originating from the solar wind (middle panel) is very similar to that of the warm electron population detected around comet 67P by the RPC-MIP instrument. This does not mean that the warm electron population is entirely composed of solar wind electrons, but rather suggests that electrons (either from the solar wind or from the ionization of cometary neutrals that occurred far from the nucleus) present a clear increase in temperature where the density is high. This is a signature of electrons that have been accelerated by the ambipolar electric field.

7. Conclusion

The cometary plasma around comet 67P has been characterized based on the response of the mutual impedance experiment of the Rosetta mission RPC-MIP. We focused on the last nine months of the mission, when the location of the Rosetta orbiter around comet 67P and the experimental conditions for the mutual impedance probe were most appropriate for extracting plasma parameters in the inner coma of comet 67P. It was possible to characterize the plasma after a compliant electrostatic modeling of the probe had been achieved, which allowed us to set up a simulated responses database. This database was then compared with the experimental responses of the probe. As a result, the mutual impedance probe responses provided by the RPC-MIP instrument that presented a high enough signal-to-noise ratio were found to be consistent with the presence, in the ionized environment of comet 67P, of two well-defined electron populations. We modeled the velocity distribution function of these populations with a double Maxwellian. Based on the available plasma parameter range (fig. 3), we found that the coldest electron population was most of the time denser than the hottest population, but it remains possible that because of the noise, undetected higher proportions of warm electrons have occurred at comet 67P, especially because a majority of the experimental responses did not show a clear plasma signature emerging from the instrument noise. A significant correlation between the warm and cold electron temperatures in the cometary plasma of comet 67P as been observed, associated with a dependence on the local cometary neutral density. The occurrence of two (cold and warm) electron populations in the close ionized environment of comet 67P, which has previously been reported in Eriksson et al. (2017), Engelhardt, I. A. D. et al. (2018), Wattieaux, G. et al. (2019) and Gilet et al. (2017), is confirmed. We also quantified the characteristics of each populations during almost half of the Rosetta cometary measurements, until end of operations. This is the core result of this study. These new observables have enabled us to investigate the relation that links the density and the temperature of the electron in the inner coma of comet 67P. On the one hand, the observed warm electron component is attributed to the ionization of the expanding cometary neutral atmosphere through photoionization (Vigren et al. 2016) and/or electron impact ionization (Galand et al. 2016; Heritier, K. L. et al. 2018), providing electrons with energies in the range 2-10 eV according to our analysis. This is consistent with theoretical
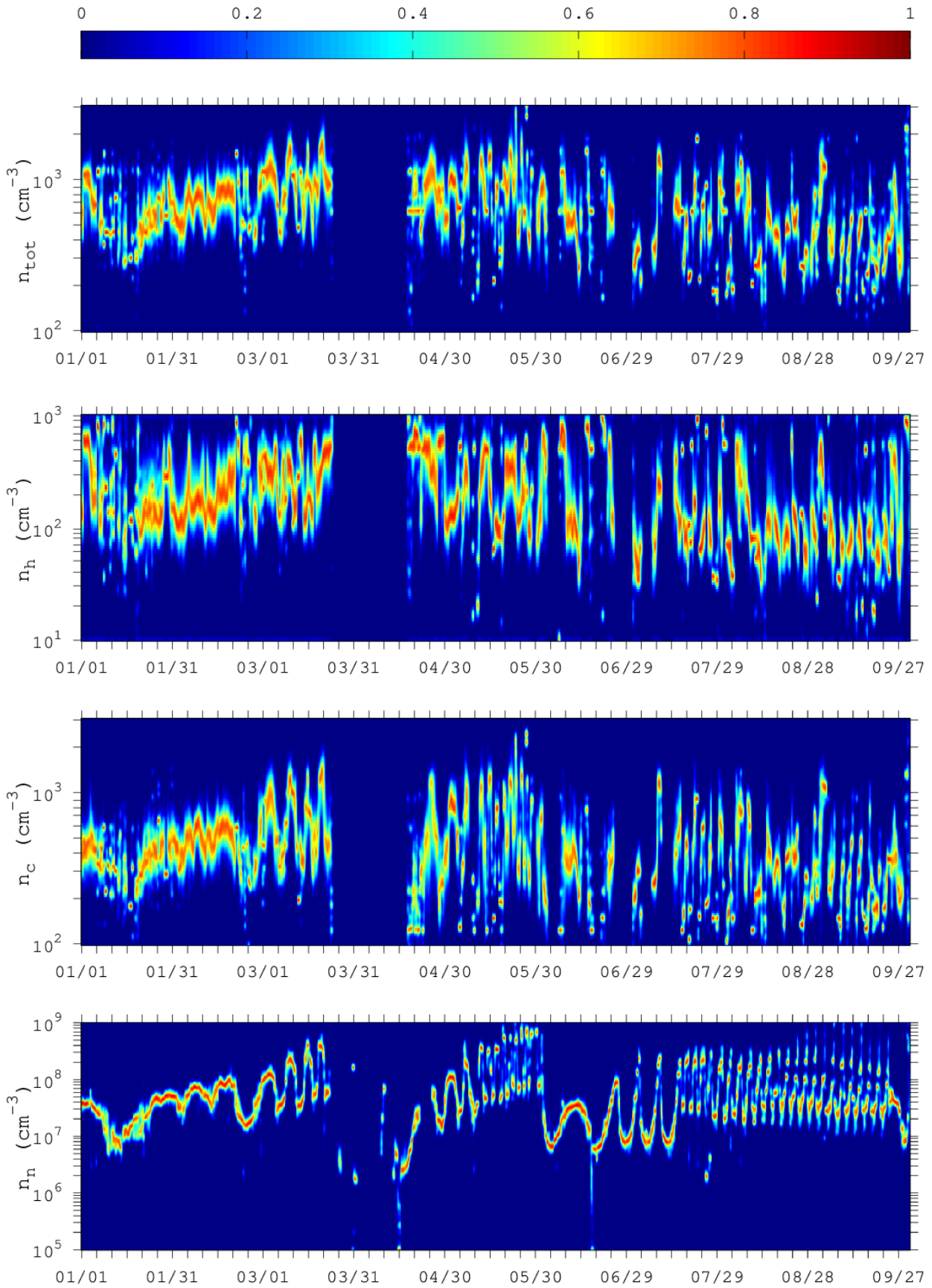
Fig. 9. Evolution of the electron densities and cometary neutral density at the Rosetta spacecraft orbiter locations around comet 67P from January to September 2016. The dispersion of the results was computed and normalized over time intervals of 6h. The neutral density has been determined from the Rosina/COPS experiment. The color bar represents the occurrence.
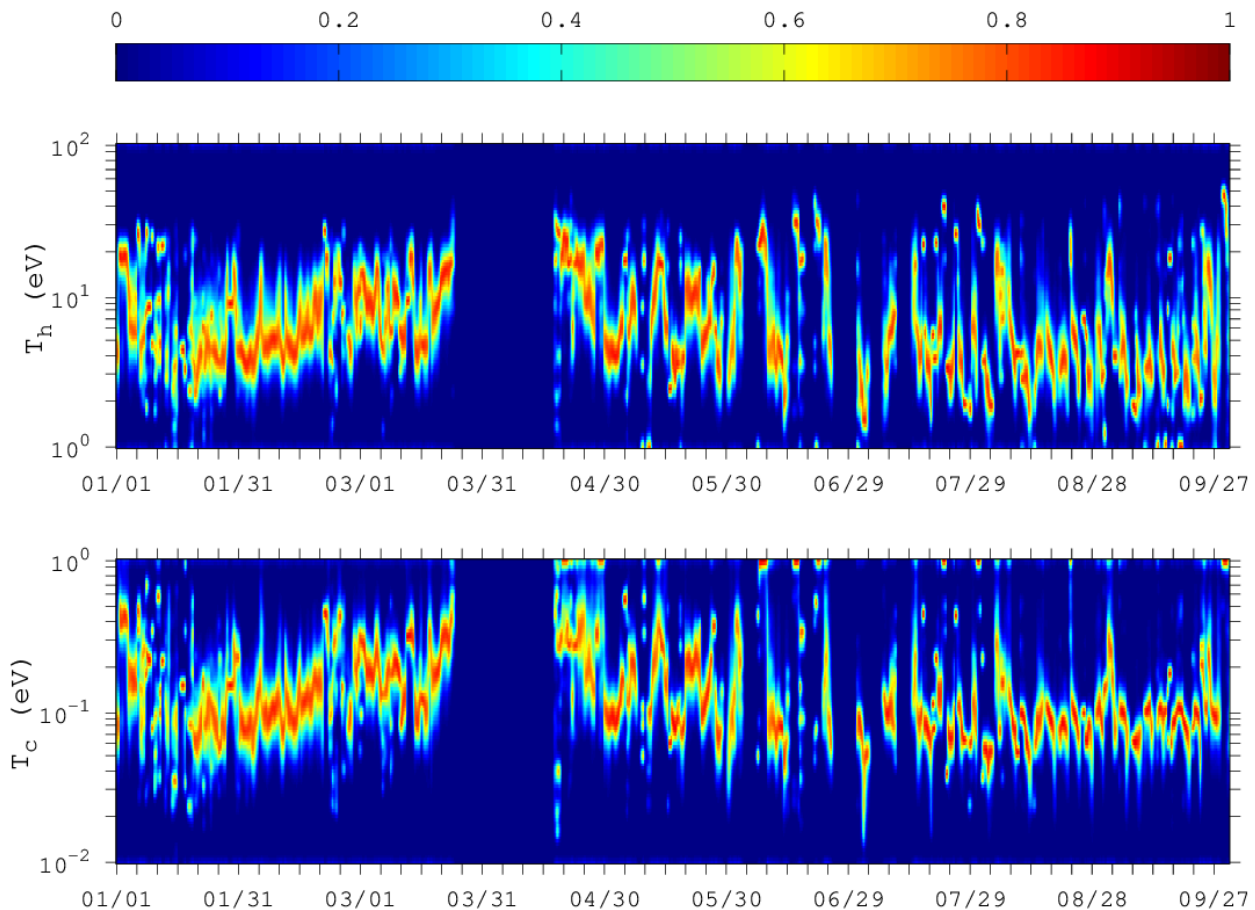
Fig. 10. Evolution of the electron temperatures at the Rosetta spacecraft orbiter locations from January to September 2016. The dispersion of the results was computed and normalized over time intervals of 6h. The color bar represents the occurrence.

expectations. On the other hand, the cold electron population is consistent with electrons that have cooled down by collisions on cometary neutral molecules (essentially H_2O and CO_2) to lower energies (0.05–0.3 eV according to this work). It is surprising that cold electrons have been found at large distances (3.6 UA) from the Sun because the so-called electron exobase (Mandt et al. 2016), which represents the region around comet 67P where the electron dynamics is expected to be dominated by collisions on neutrals, was not expected to have formed during the last months of cometary operations. Finally, even though the responses of the RPC-MIP experiment that exhibited a clear plasma signature were always different from simulations including a single Maxwellian eedf, many experimental responses that did not show a plasma signature emerging from the noise might have been related to a Maxwellian eedf.

References

Balsiger, H., Altwegg, K., Bochsler, P., et al. 2007, Space Science Reviews, 128, 745
Beck, A. & Pantellini, F. 2008, Plasma Physics and Controlled Fusion, 51, 015004
Beghin, C. 1995, Radio Science, 30, 307
Beghin, C. & Debrie, R. 1972, Journal of Plasma Physics, 8, 287
Beghin, C., Debrie, R., Berthelier, J. J., et al. 1982, Advances in Space Research, 2, 61
Béghin, C., Décréau, P. M. E., Pickett, J., Sundkvist, D., & Lefebvre, B. 2005, Radio Science, 40, RS6008
Behar, E., Nilsson, H., Henri, P., et al. 2018, A&A, 616, A21
Chasseriaux, J. M., R. Debrie, R. D., & C. Renard, C. R. 1972, Journal of Plasma Physics, 8, 231
Deca, J., Divin, A., Henri, P., et al. 2017, Phys. Rev. Lett., 118, 205101
Deca, J., Henri, P., Divin, A., et al. 2019, Phys. Rev. Lett., 123, 055101
Décréau, P., Béghin, C., & Parrot, M. 1978, Space Science Reviews, 22, 581
Edberg, N. J. T., Eriksson, A. I., Odelstad, E., et al. 2015, Geophysical Research Letters, 42, 4263
Engelhardt, I. A. D., Eriksson, A. I., Vigren, E., et al. 2018, A&A, 616, A51
Eriksson, A. I., Engelhardt, I. A., André, M., et al. 2017, Astronomy and Astrophysics - A&A
Galand, M., Heritier, K. L., Odelstad, E., et al. 2016, Monthly Notices of the Royal Astronomical Society, 462, S331
Geiswiller, J., Béghin, C., Kolesnikova, E., et al. 2001, Planetary and Space Science, 49, 633
Gilet, N., Henri, P., Wattieaux, G., Cilibrasi, M., & Béghin, C. 2017, Radio Science, 52, 1432, 2017RS006294
Gilet, N., Henri, P., Wattieaux, G., et al. 2019a, Frontiers in Astronomy and Space Sciences, 6, 16
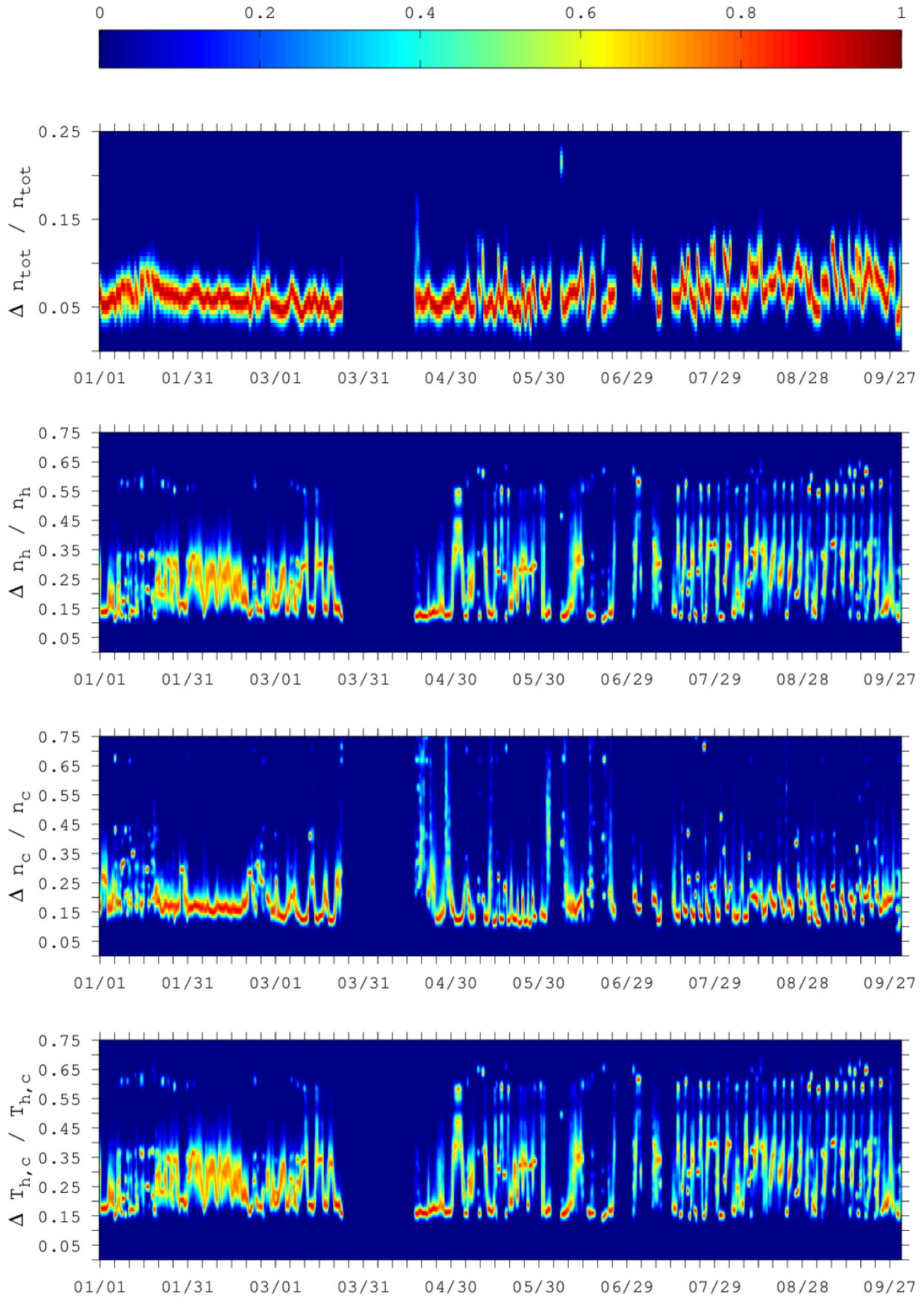Gilet, N., Henri, P., Wattieaux, G., et al. 2019b, Astronomy and Astrophysics, (submitted)

Fig. 11. Relative uncertainties on the plasma parameters from January to September 2016. The color bar represents the occurrence.
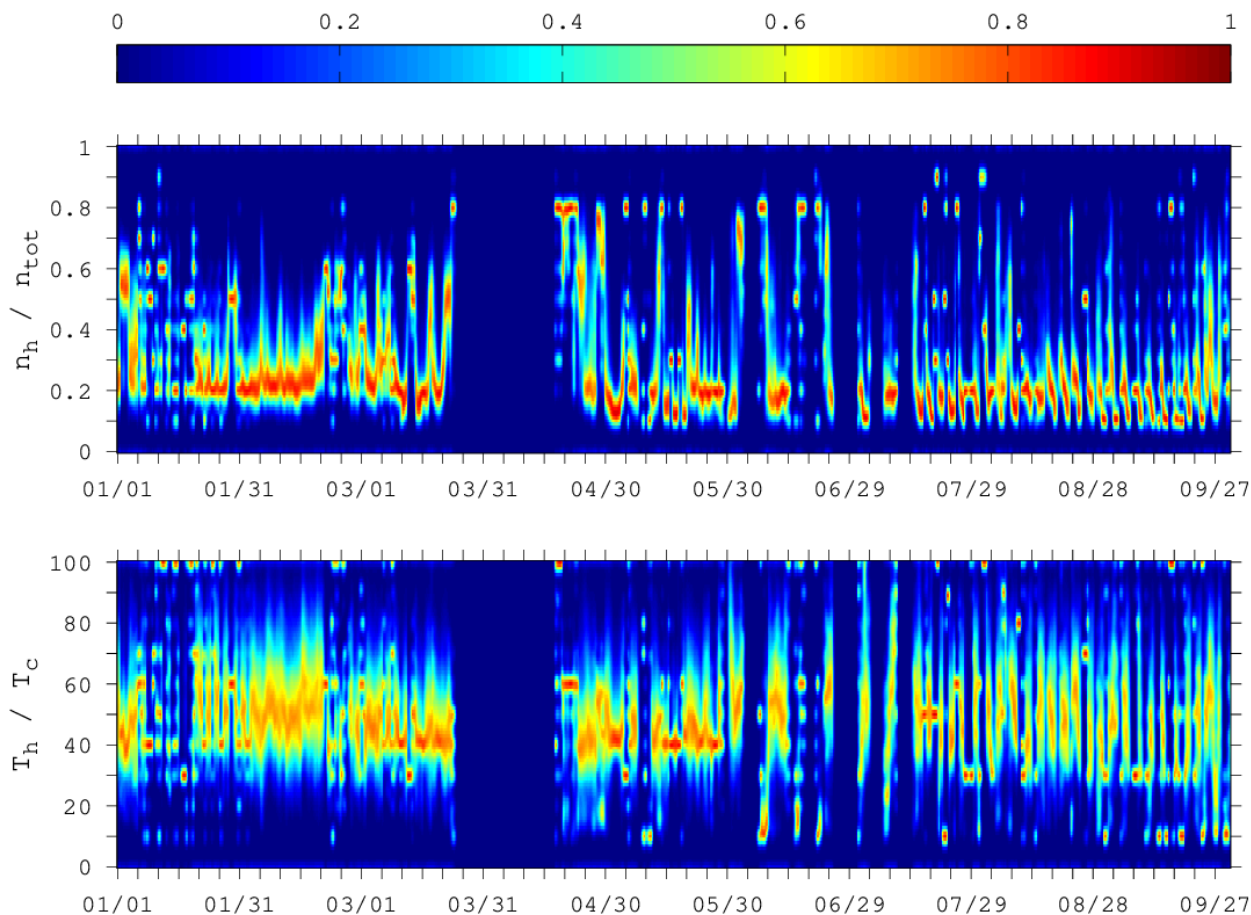
Fig. 12. Evolution of the density and temperature ratio at the Rosetta spacecraft orbiter locations from January to September 2016. The dispersion of the results was computed and normalized over time intervals of 6h. The color bar represents the occurrence.

Grard, R. 1969, Alta Freq., 38, 97

Grard, R. 1997, Radio Science, 32, 1091

Henri, P., Valliéres, X., Lagoutte, D., & Traore, N. 2018, ROSETTA-ORBITER 67P RPCMIP 3 xxxx V2.0, RO-C-RPCMIP-3-xxxx-V2.0, ESA Planetary Science Archive and NASA Planetary Data System

Henri, P., Valliéres, X., & RPC-MIP team. 2019, User Guide to the RPC-MIP Science Datasets in the ESA's Planetary Science Archive (PSA), RPC-MIP-UG-LPC2E

Heritier, K. L., Galand, M., Henri, P., et al. 2018, A&A, 618, A77

Madanian, H., Cravens, T. E., Rahmati, A., et al. 2016, Journal of Geophysical Research: Space Physics, 121, 5815

Mandt, K. E., Eriksson, A., Edberg, N. J. T., et al. 2016, Monthly Notices of the Royal Astronomical Society, 462, S9

Meyer-Vernet, N., Couturier, P., Hoang, S., et al. 1986, Science, 232, 370

Murakami, M. & Basko, M. M. 2006, Physics of Plasmas, 13, 012105

Odelstad, E., Eriksson, A. I., Edberg, N. J. T., et al. 2015, Geophysical Research Letters, 42, 10

Pottelette, R., Rooy, B., & Fiala, V. 1975, Journal of Plasma Physics, 14, 209

Pottelette, R. & Storey, L. R. O. 1981, Journal of Plasma Physics, 25, 323

Rooy, B., Feix, M. R., & Storey, L. R. O. 1972, Plasma Physics, 14, 275

Storey, L. R. O. 1998, Washington DC American Geophysical Union Geophysical Monograph Series, 103, 155

Storey, L. R. O., Aubry, M. P., & Meyer, P. 1969, in Plasma Waves in Space and in the Laboratory, ed. J. O. Thomas & B. J. Landmark, 303

Trotignon, J. G., Michau, J. L., Lagoutte, D., et al. 2007, Space Science Reviews, 128, 713

Vigren, E., Altwegg, K., Edberg, N. J. T., et al. 2016, The Astronomical Journal, 152, 59

Volwerk, Martin, Goetz, Charlotte, Richter, Ingo, et al. 2018, A&A, 614, A10

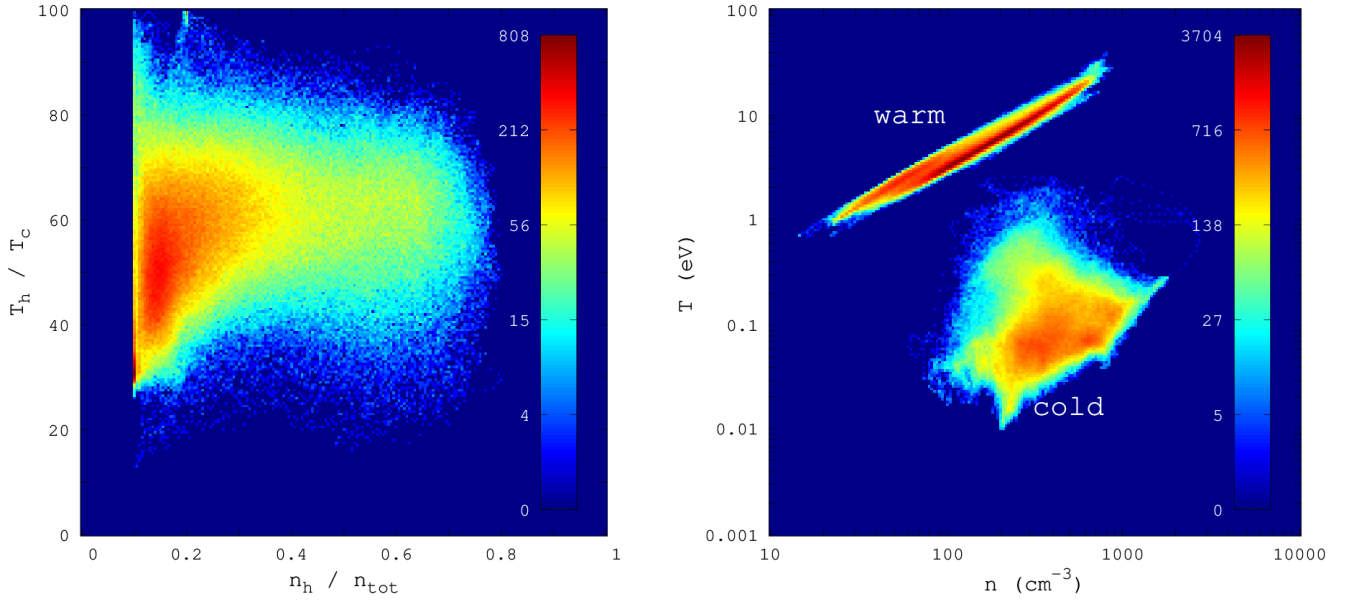Wattieaux, G., Gilet, N., Henri, P., Vallières, X., & Bucciantini, L. 2019, A&A, 630, A41

Fig. 13. Distribution of T_h/T_c vs. n_h/n_{tot} (left) and of the electron temperatures vs. the electrons densities (right) estimated at the Rosetta orbiter locations in the cometary plasma of comet 67P from January to September 2016 (570000 samples). Colors correspond to the number of responses (the color map is logarithmically scaled in both panels).
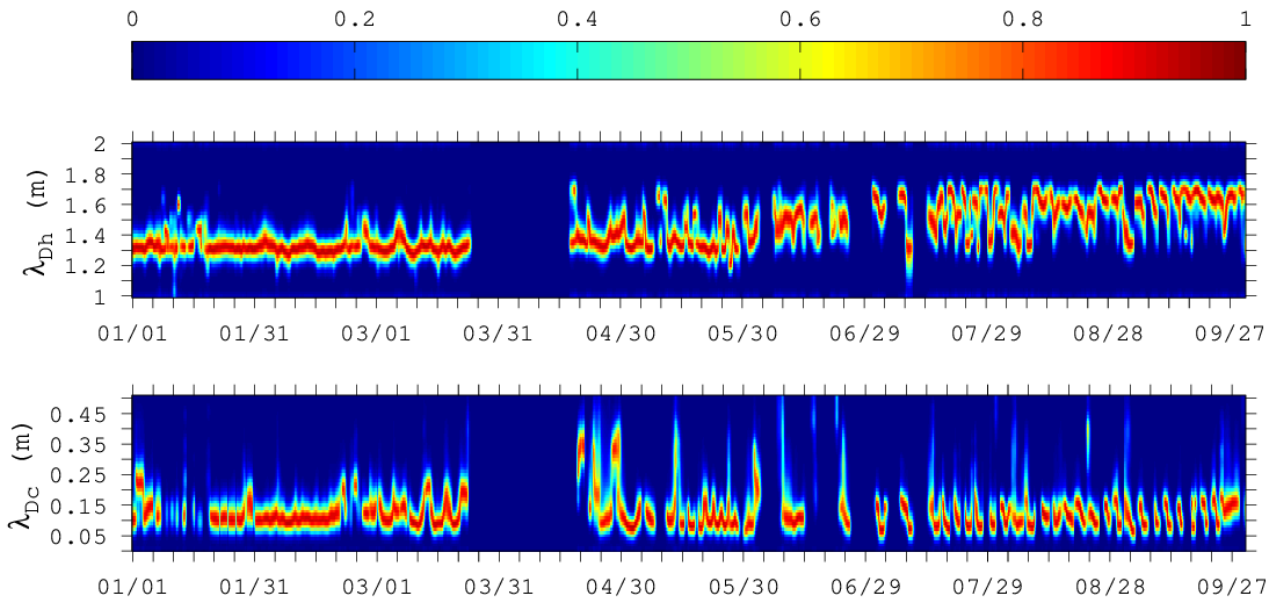

Fig. 14. Evolution of the warm (λ_{Dh}) and cold (λ_{Dc}) Debye length at the Rosetta spacecraft orbiter locations from January to September 2016. The dispersion of the results was computed and normalized over time intervals of 6h. The color bar represents the occurrence.
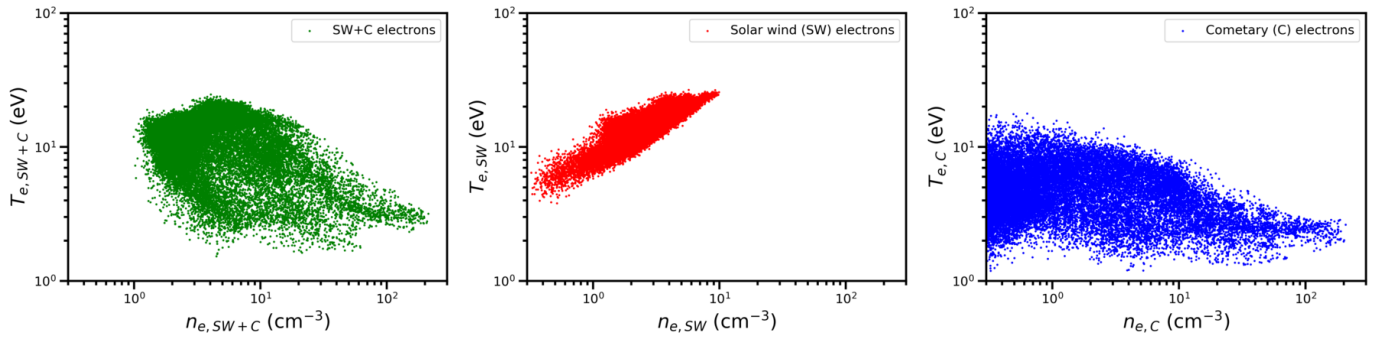
Fig. 15. Electron density vs. temperatures from kinetic numerical simulations of the interaction between the solar wind and a comet. Left panel: Temperature and density computed for the total electron population. Middle panel: Temperature and density computed for the solar wind electron population. Right panel: Temperature and density computed for the cometary electron population.